

Supporting Information for

**Ultrathin g-C₃N₄ nanosheets coupled with amorphous Cu doped FeOOH
nanoclusters as 2D/0D heterogeneous catalysts for water remediation**

Shouwei Zhang,^{ab} Huihui Gao,^{ab} Yongshun Huang,^c Xiangxue Wang,^b Tasawar Hayat,
^d Jiaxing Li,^{*cd} Xijin Xu,^{*a} Xiangke Wang^{*b}

^a School of Physics and Technology, University of Jinan, P. R. China, E-mail:
sps_xuj@ujn.edu.cn

^b School of Environmental Science and Engineering, North China Electric Power
University, Beijing 102206, PR China, E-mail: xkwang@ncepu.edu.cn

^c CAS Key Laboratory of Photovoltaic and energy conservation materials, Institute of
Plasma Physics, Chinese Academy of Sciences, P.O. Box 1126, 230031 Hefei, P. R.
China, E-mail: lijx@ipp.ac.cn

^d NAAM Research Group, Department of Mathematics, Faculty of Science, King
Abdulaziz University, Jeddah, Saudi Arabia

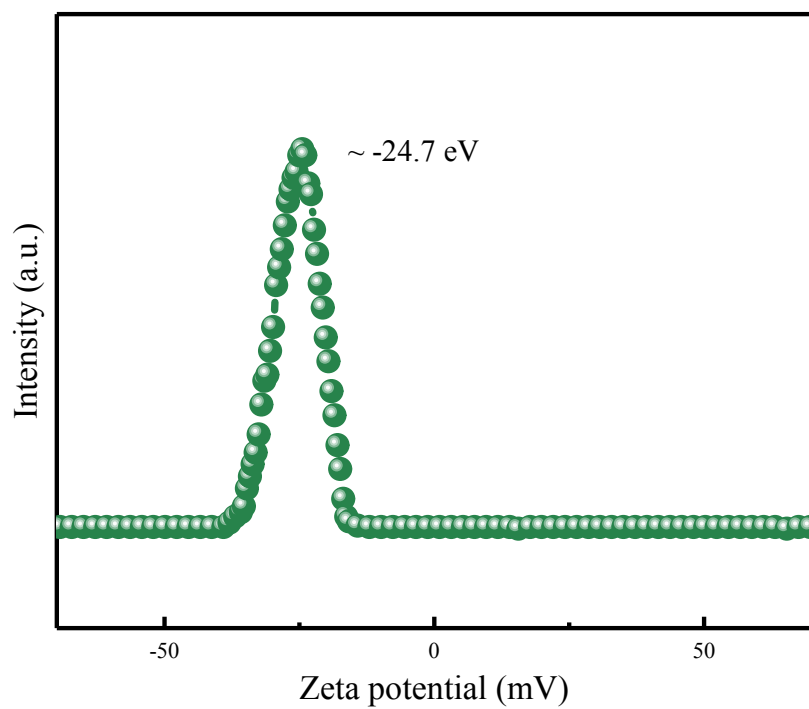


Figure S1. The surface of CNNS is negatively charged with a Zeta potential of -24.7 mV.

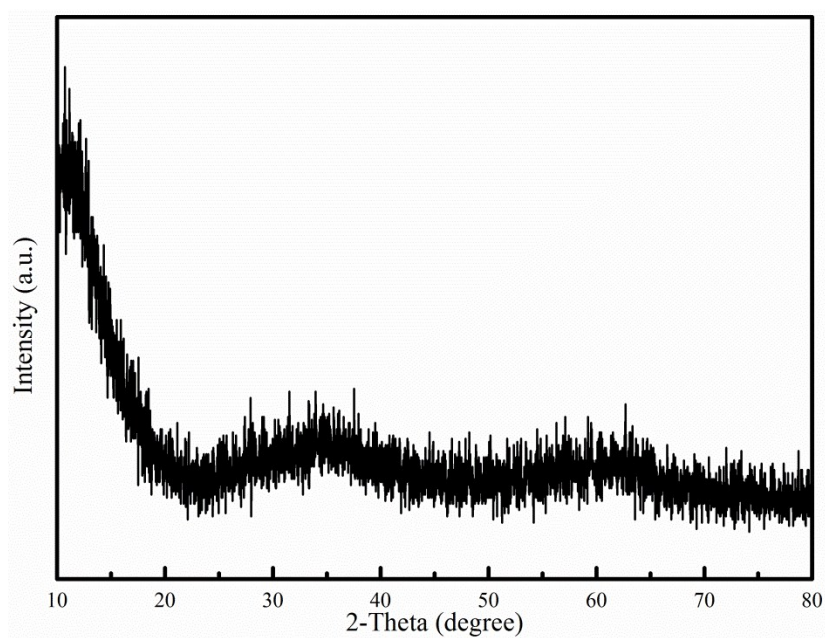


Figure S2. XRD pattern of Cu-FeOOH clusters.

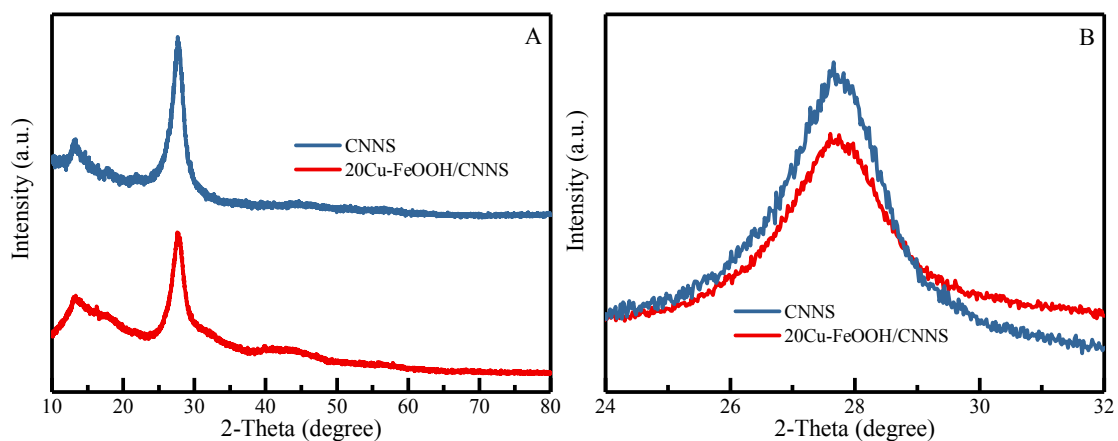


Figure S3. (A) XRD patterns of CNNS and 20Cu-FeOOH/CNNS; (B) The magnified in the range of $2\theta = 24\text{-}32^\circ$.

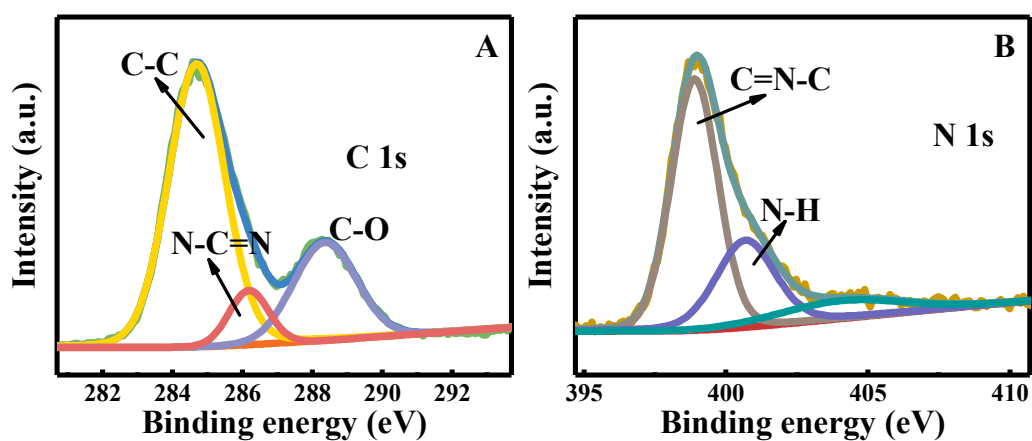


Figure S4. XPS spectra of 20Cu-FeOOH/CNNS. C 1s (A) and N 1s (B).

The catalysts CNNS, Cu-FeOOH, FeOOH/CNNS, 5FeOOH/CNNS ~ 30Cu-FeOOH/CNNS removed ~9.2, ~9.3, ~11.5, ~12.5, ~14.9, ~16.5 and ~18.1%, respectively, of MB after 30 min of adsorption in the dark (Fig. S5). Upon 40 min of reaction under dark condition, the adsorption of MB reached ~9.3, ~9.5, ~11.1, ~12.6, ~13.9, ~16.3 and ~17.7% for CNNS, Cu-FeOOH, FeOOH/CNNS, 5FeOOH/CNNS ~ 30Cu-FeOOH/CNNS, respectively. No absorption efficiency differences was observed, indicating an adsorption/desorption equilibrium of the MB within 30 min.

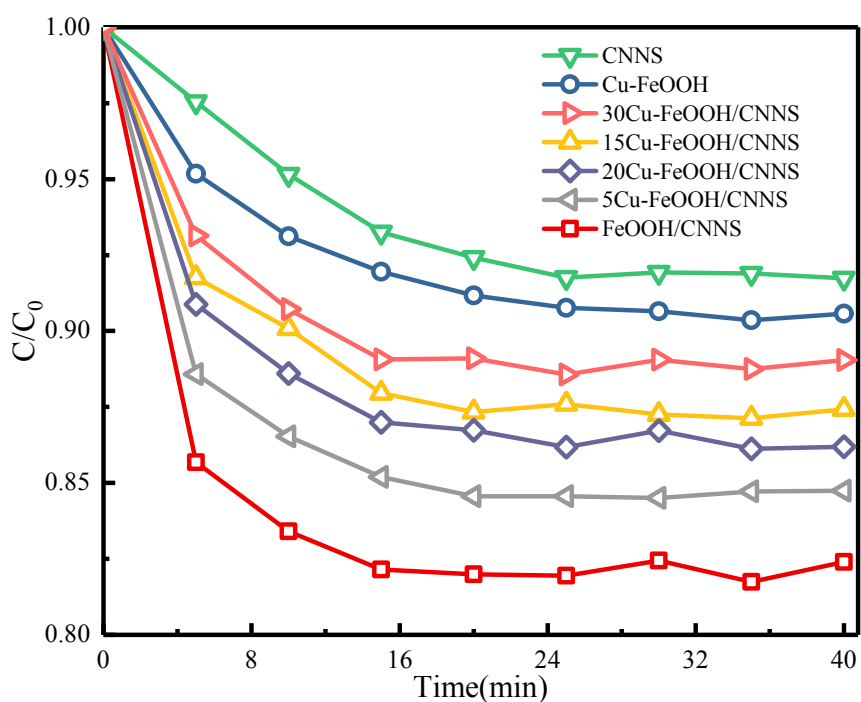


Figure S5. Adsorption properties of MB over as-prepared catalysts in dark.

H_2O_2 concentration was detected by reported DPD/POD method.¹ According to the mechanism, N,N-diethyl-p-phenylenediamine (DPD) can be oxidized by H_2O_2 to higher valence using horseradish peroxidase (POD) as a catalyst. The radical cation ($\text{DPD}\cdot+$) produced from the oxidation of two DPD molecules exhibits two absorption maxima at ~ 510 and 551 nm. As shown in Fig. S6, the concentration of H_2O_2 decreased quickly after reaction for 40 min. The low concentration of H_2O_2 contributed to the rapid and complete decomposed by 20Cu-FeOOH/CNNS. These results suggested that MB degradation is essentially accomplished by a heterogeneous catalytic photo-Fenton process.

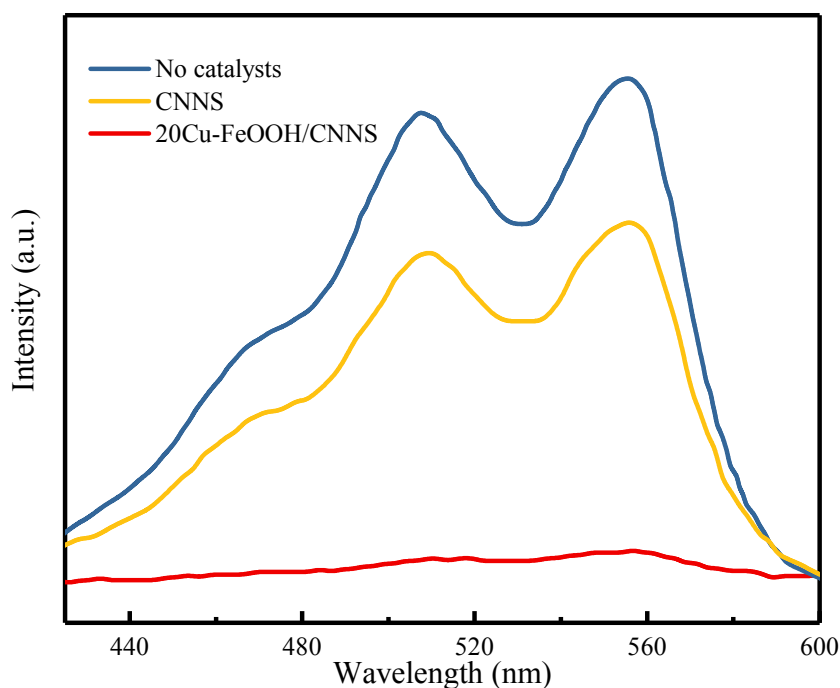


Figure S6. Detection of H_2O_2 concentration for the solution after 40 min illumination over different catalysts, using a DPD/POD method.

1. H. Bader, V. Sturzenegger, J. Hoigne, Water Res. 22 (1988) 1109-1115.

We conducted Fenton and photo-Fenton reaction over 20Cu-FeOOH/CNNS, as showed in Fig. S7. Fenton effect slightly reduced the concentration of MB, while photo-Fenton effect had a profound impact on degradation of MB, and it is almost able to completely degrade MB within 40 min. The catalytic activity of photo-Fenton reaction was much higher than 20Cu-FeOOH/CNNS.

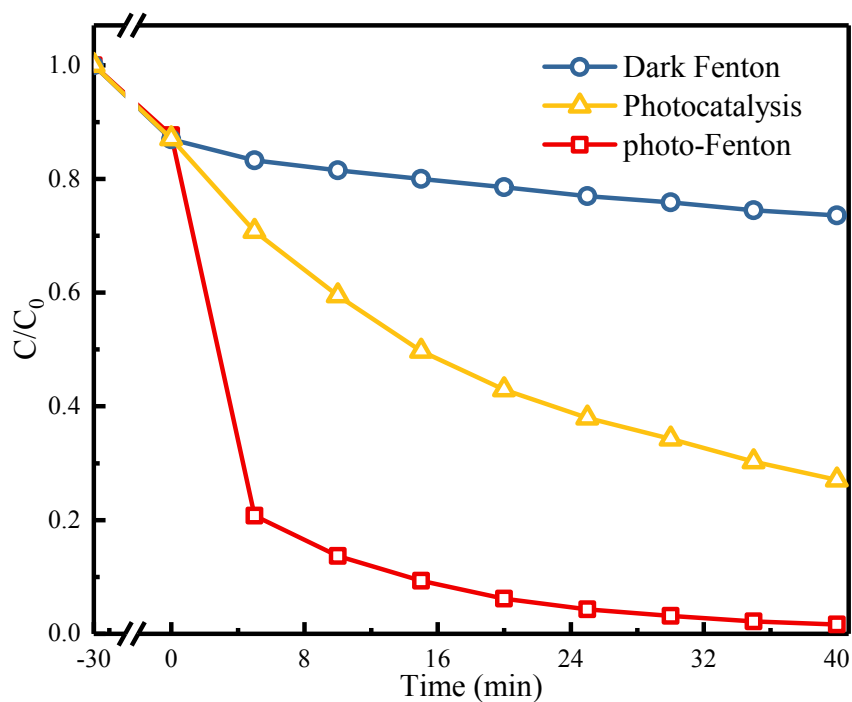


Figure S7. Effect of Fenton and photo-Fenton reaction over the 20Cu-FeOOH/CNNS on degradation of MB.

Fig. S8A showed MB degradation via catalytic photo-Fenton process with different catalysts. When CNNS and FeOOH/CNNS are employed as the catalysts, MB degradation can be increased to ~44.3% and ~63.3% in 40 min, respectively. It is very interesting that with the appearance of Cu doping, Cu-FeOOH/CNNS contribute to more powerful MB degradation, and the degradation efficiencies can reach up to ~98.7% in 40 min. Even within 5 min, its degradation efficiency is still ~80.3%, indicating the excellent photo-Fenton activity of Cu-FeOOH/CNNS. By considering the features of Cu-FeOOH/CNNS, there are several important factors, e.g. Cu/CNNS, FeOOH/CNNS, Cu-FeOOH and the synergistic effect between Cu, FeOOH and CNNS, which may be responsible for the significant enhancement in catalytic ability. The direct contribution from Cu doping in Cu/CNNS can be easily excluded because individual doping fabricated by the similar method only presents MB degradation at ~49.6% in 40 min, which is very close to the degradation efficiency in CNNS system (44.3%, Fig. S8A). The negligible increase of MB removal in Cu/CNNS system may be attributed to the weak Fenton catalytic activity on the surface of Cu doping. Similarly, the direct contribution from CNNS is easily evaluated, Cu-FeOOH exhibited degradation efficiencies of ~55.4%, suggesting that CNNS played a critical role in the enhancement of photocatalytic activity. Moreover, dramatic enhancement in the degradation of MB is observed through the simultaneous introduction of Cu and FeOOH. Nearly ~98.7% of MB is degraded within 40 min under visible light irradiation, indicating the presence of a synergetic catalytic effect among Cu, FeOOH and CNNS in the Cu-FeOOH/CNNS system, thereby enhancing the relative rates of mass transfer to reactive sites and

chemical reaction at reactive sites.

We also conduct a series of controlled experiments. By fixing the amount of $\text{FeCl}_3 \cdot 6\text{H}_2\text{O}$ and ethanol at 1 mmol and 40 mL, respectively, the starting amount of CNNS precursor was set at 300, 500, 700 and 900 mg, respectively. The corresponding products after reaction were denoted as FeOOH/CNNS-300, FeOOH/CNNS-500, FeOOH/CNNS-700 and FeOOH/CNNS-900, respectively. The preliminary studies showed that the FeOOH/CNNS-700 without Cu doping exhibited the highest photocatalytic degradation rate under visible light irradiation (Fig. S8B). Therefore, this composition (FeOOH/CNNS-700) was chosen in the current study.

Based on these results, it can be concluded that the synergistic effect between Cu, FeOOH and CNNS may be helpful to improve the activation of H_2O_2 , but the enhanced catalytic activity in Cu-FeOOH/CNNS should be more dependent on the simultaneous optimizations of surface property and the microstructure induced by Cu doping.

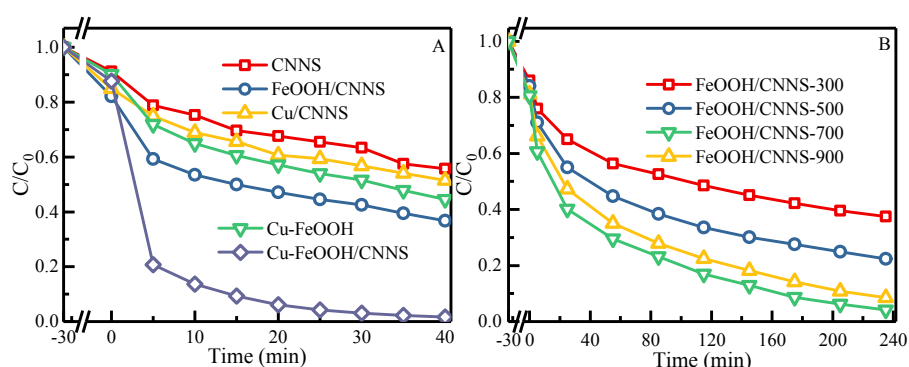


Figure S8. (A) The catalytic activity of the different catalysts under visible light irradiation; (B) the influence of CNNS contents on the removal efficiency of MB.

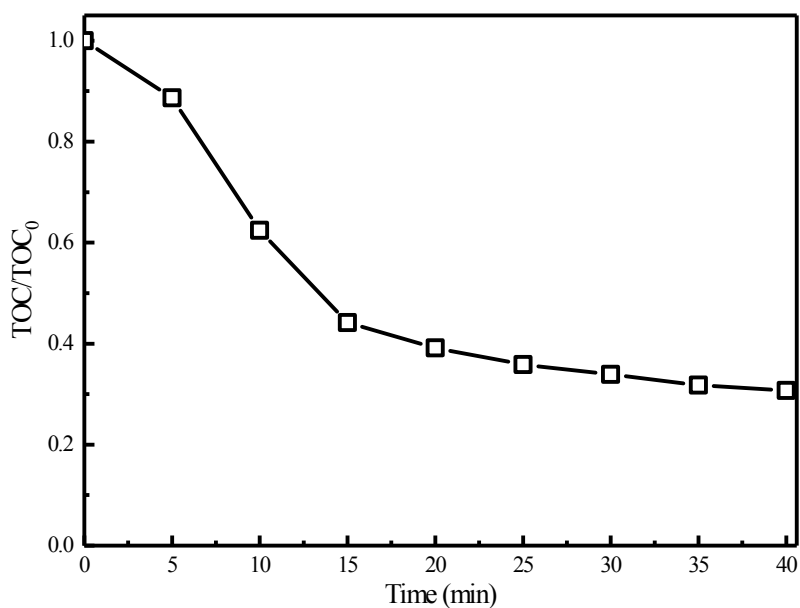


Figure S9. TOC removal during the degradation of MB.

The effects of catalyst dosage on MB degradation were further evaluated (Fig. S10). The degradation efficiency of MB increases from ~76.5% with 5 mg/L of catalyst to ~96.9% with 30 mg/L of catalyst within 10 min, suggesting that the increased loading of catalyst provides more active sites for H₂O₂ to interact with the 20Cu-FeOOH/CNNS. However, further increasing the catalyst loading does not noticeably improve the MB removal efficiency due to the limited dye concentration.

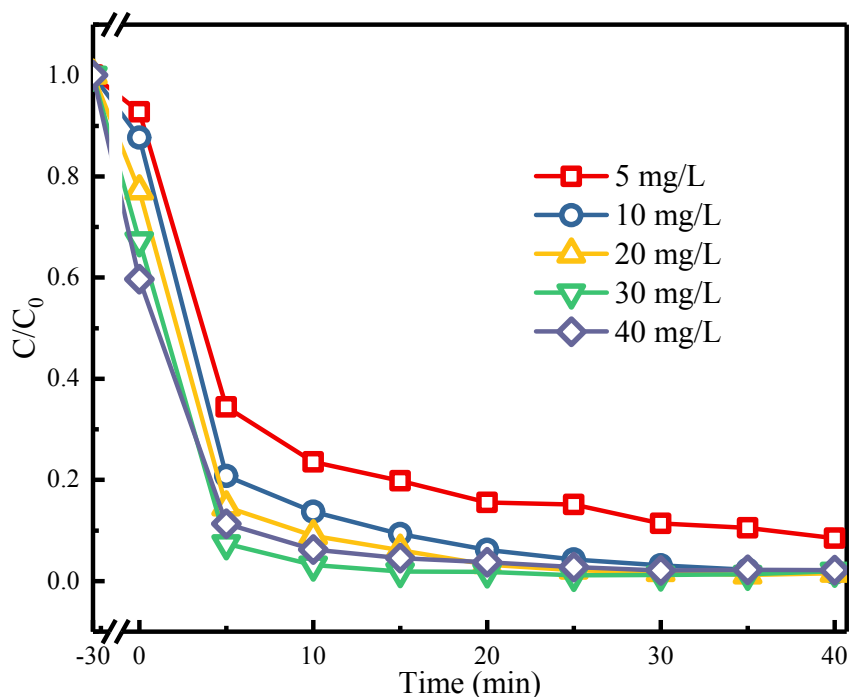


Figure S10. The effect of catalyst dosage on MB degradation.

To verify the role of O_2 in this PFR, the reaction solution infused with N_2 and O_2 was investigated (Fig. S11A). The results indicated that higher dissolved O_2 levels resulted in more fast degradation kinetic rate, while the degradation rate of MB was inhibited after being pumped with N_2 . These results revealed that O_2 played a significant role in this PFR. Moreover, the addition of BQ used as an efficient trapper of $O_2^{\cdot-}$, the degradation of MB could be slightly limited, which indicated that only a small amount of $O_2^{\cdot-}$ might participate in MB degradation. Moreover, MB degradation with the different pH was also conducted, as displayed in Fig. S11B. It was found that the degradation efficiency largely increased with reducing pH value. The results indicated that H_2O_2 was used as the intermediate oxidation reagent. When the moderate $O_2^{\cdot-}$ produced from dissolved O_2 , as H^+ existed, it would assist $O_2^{\cdot-}$ to react with electron to form H_2O_2 . That is, H_2O_2 concentration may increase through the direct interactions

of photogenerated electrons with the surface adsorbed oxygen on the photocatalyst under Cu-FeOOH/CNNS+O₂+sunlight system, and leading to enhancement of degradation rate.

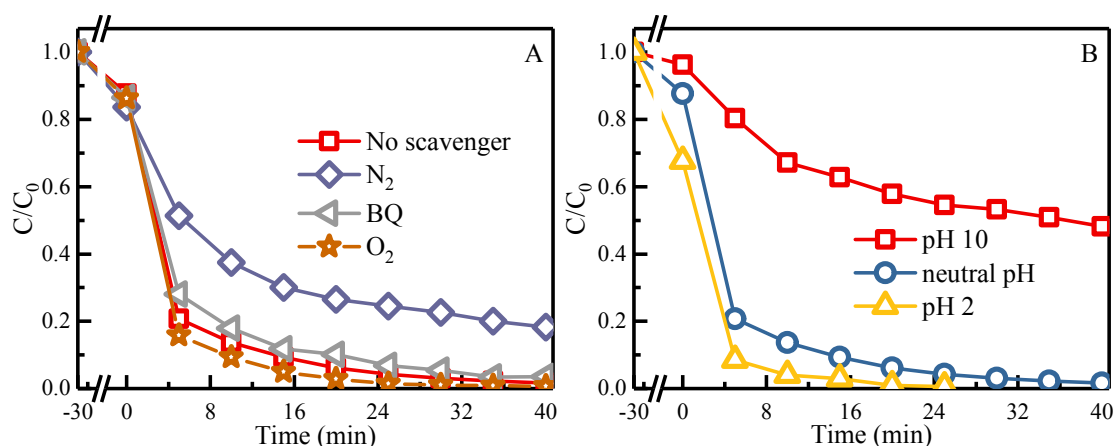
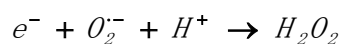


Figure S11. (A) The degradation of MB in the presence of different scavengers (A) and (B) in different pH value.

The electron spin resonance (ESR) technique with 5,5-dimethyl-1-pyrroline-N-oxide (DMPO) as a radical trapping agent was carried out to examine the radical species that were generated during the 20Cu-FeOOH/CNNS catalytic process. As shown in Fig. S12, negligible ESR signals are observed under dark conditions. However, the intensity ratio of 1:1:1:1 quartet characteristic ESR signals for DMPO-O₂^{·-} and a 1:2:2:1 quarter pattern signals for the DMPO-·OH spin adduct are found under visible light irradiation for 10 min. This suggested that O₂^{·-} and ·OH are generated in both CNNS and 20Cu-FeOOH/CNNS catalytic systems. Moreover, the DMPO-·OH signals of the 20Cu-FeOOH/CNNS are significantly stronger than that of the CNNS, which revealed that

more $\cdot\text{OH}$ radical species could be generated following the introduction of Cu-FeOOH, while the DMPO- $\text{O}_2^{\cdot-}$ signals are only slightly increase in the presence of 20Cu-FeOOH/CNNS. That is to say, 20Cu-FeOOH/CNNS plays a crucial role in activating hydrogen peroxide to generate large amounts of $\cdot\text{OH}$ under current conditions. This was consistent with the results that $\cdot\text{OH}$ was major oxidation active species.

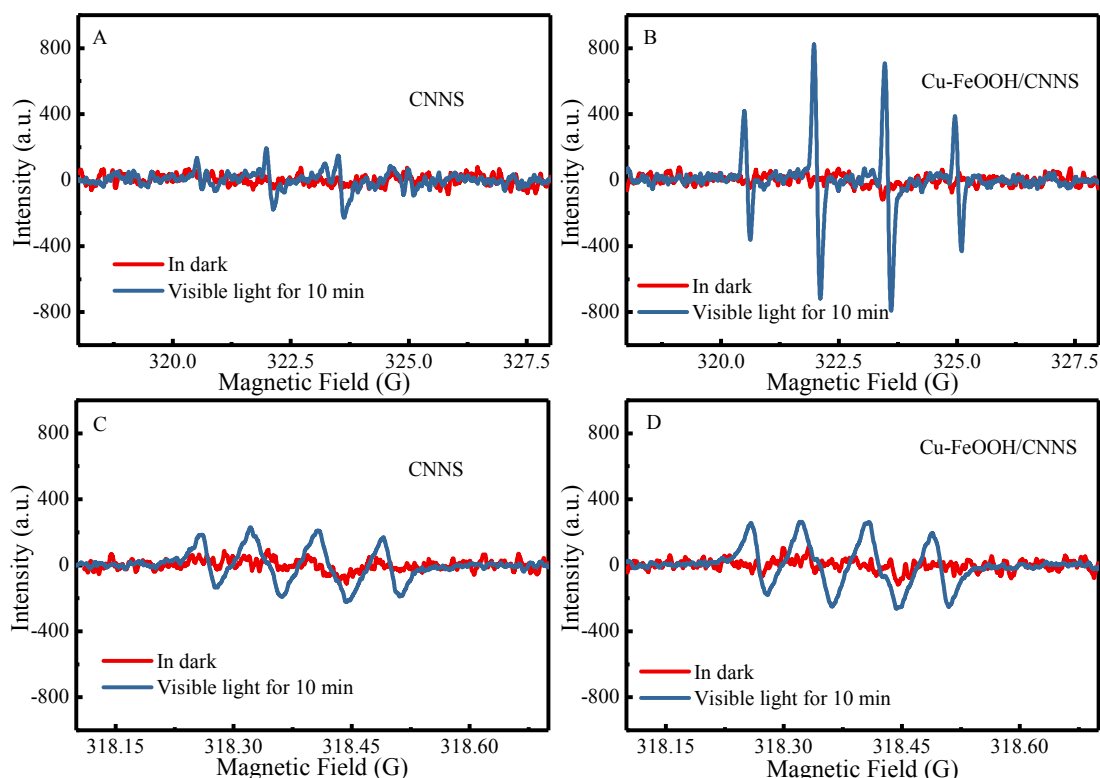


Figure S12. The ESR spectra of the (A and B) DMPO- $\cdot\text{OH}$ adducts, (C and D) DMPO- $\text{O}_2^{\cdot-}$ adducts, recorded with the CNNS and 20Cu-FeOOH/CNNS under visible light irradiation.

The stability and reusability of the catalysts is crucial to their practical applications. The catalytic stability of 20Cu-FeOOH/CNNS composite was also studied by recycling the catalytic degradation of MB under the same conditions, as shown in Fig. S13A. It is interesting to find that no obvious decrease in the catalytic efficiency of 20Cu-

FeOOH/CNNS composite is observed in MB degradation after ten recycles, suggesting that this catalyst have good reusability and have great potential in their practical application. The good stability could be ascribed to the dynamic equilibrium of $\text{Fe}^{3+}/\text{Fe}^{2+}$ and $\text{Cu}^{2+}/\text{Cu}^+$ under the visible light radiation. To further evaluate the stability of the 20Cu-FeOOH/CNNS, the metal leaching in the 1st, 5th and 10th cycles were measured by Atomic Absorption Spectroscopy, and the results are plotted in Fig. S13B. It is clear that the concentrations of dissolved metal ions are low, reaching a value of ~ 0.597 and ~ 0.341 mg/L for Cu^{2+} and Fe^{2+} in the 1st cycle, respectively. In the following cycles, the level of metal leaching shows a downward trend, with the concentration of leached Cu^{2+} and Fe^{2+} being only ~ 0.246 and ~ 0.093 mg/L in the 10th cycle, respectively. In order to evaluate the effect of Cu^{2+} and Fe^{2+} leached from the catalyst, CuSO_4 and Fe_2SO_4 were selected as the source of Cu^{2+} and Fe^{2+} , which are important reactants in the Fenton reaction. The concentrations of Cu^{2+} and Fe^{2+} in the above reaction are 10 mg/L. As shown in Fig. S13C, the degradation ratio is only $\sim 17.6\%$ and $\sim 32.7\%$ for Cu^{2+} and Fe^{2+} in 40 min, respectively, indicating the Cu^{2+} and Fe^{2+} ions have little effect on the catalytic efficiency in our reaction system. All these analyses indicate the excellent stability and reusability of the 20Cu-FeOOH/CNNS composite. Thus, the 20Cu-FeOOH/CNNS catalyst is quite robust for applications in sewage disposal due to its high reactivity, low ion leaching, excellent long-term stability and reusability.

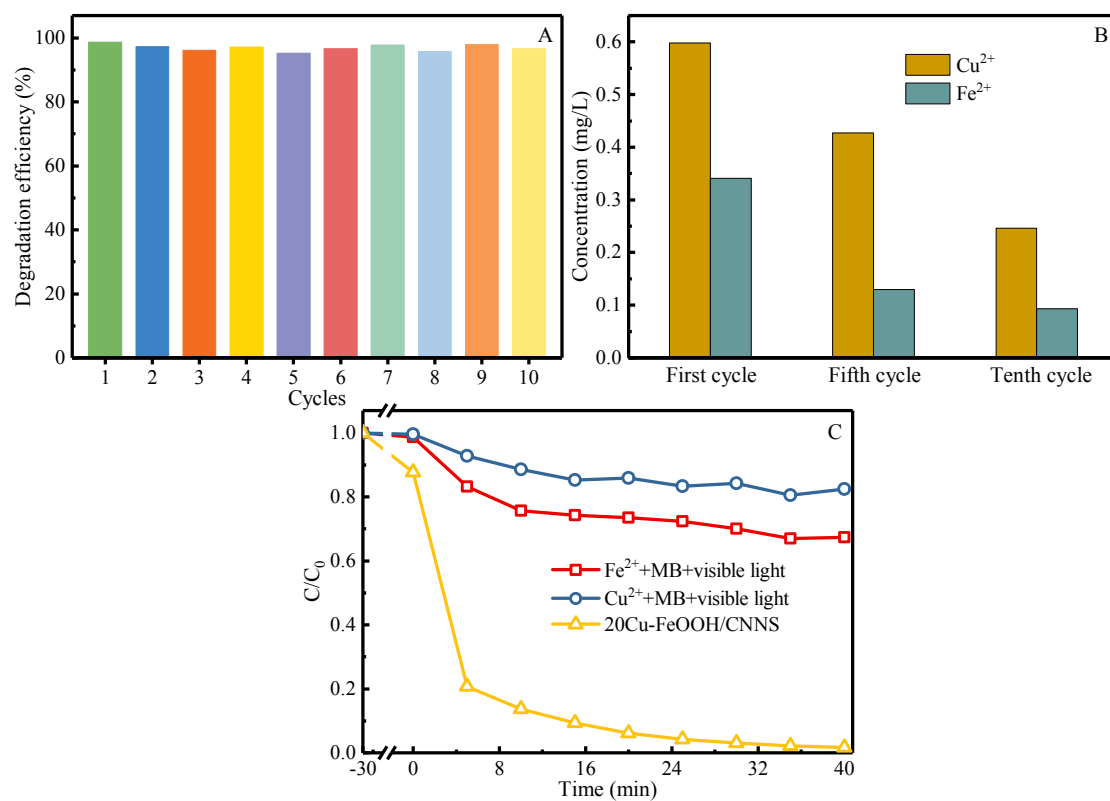


Figure S13. (A) Degradation efficiency of MB during different cycles; (B) Concentrations of dissolved Cu²⁺ and Fe²⁺ leached from the 20Cu-FeOOH/CNNS composite in the 1st, 5th and 10th cycles; and (C) photo-Fenton reaction based on CuSO₄ and Fe₂SO₄.

For a better insight into the valence state changes of Cu-FeOOH/CNNS before and after reaction, XPS analyses were carried out and shown in Fig. S14. Fig. S14A gives XPS survey spectra, which clearly showed the presence of C, N, O, Fe and Cu elements in both samples. The analysis of Fe 2p curves as shown in Figure 4B indicated that the iron species on the CNNS surface include Fe²⁺ (~711.1 eV), and Fe³⁺ (~713.4 eV), for which the atomic ratios were ~19.60%, and ~27.74%, respectively (Fig. S14B). However, after removal tests, most of the Fe existed as Fe²⁺ (~24.13%) rather than as Fe³⁺ (~19.21%), illustrating that Fe(III) species could trap one photogenerated electron and reduce to Fe(II) species.

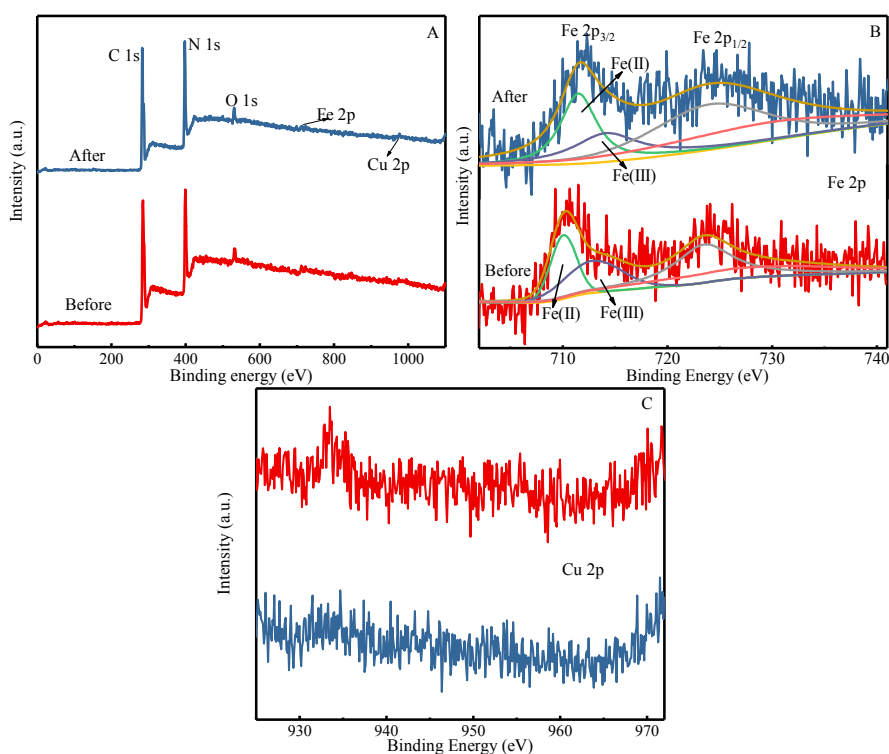


Figure S14. The XPS spectra of 20Cu-FeOOH/CNNS before and after reaction. Survey spectrum (A) and Fe 2p (B).

Table S1. The theoretical and actual molar ratio of Cu to Fe in composite.

Theoretical (molar ratio.%)	5	15	20	30
Real (molar ratio.%)	4.96	15.08	19.69	29.56

Table S2. Summary of surface areas and the catalytic activities of CNNS and 20Cu-FeOOH/CNNS catalysts as well as the catalytic activity enhancement times.

catalysts	S_{BET}	MB	
		K	K'
CNNS	~101.33	~0.011	~1.09×10 ⁻⁴
20Cu-FeOOH/CNNS	~80.94	~0.089	~1.10×10 ⁻³
Enhancement times	~0.79	~8.1	~10.09

* S_{BET} : m²/g; K: min⁻¹; K': g/(min·m²); The K' values were K values normalized with the surface areas.